Self-Assembly of a Conjugated Polymer: From Molecular Rods to a Nanoribbon Architecture with Molecular Dimensions

Paolo Samorí,[a] Viola Francke,[b] Klaus Müllen,*[b] and Jürgen P. Rabe*[a]

Abstract: The growth from solution of novel end-functionalised poly(*para*-phenyleneethynylene)s (PPEs) on flat solid crystalline substrates was investigated. The macromolecular structure of PPE at the interface between the basal plane of graphite and an organic solution was visualised with molecular resolution by scanning tunnelling microscopy. It revealed a two-dimensional nematic-like molecular order of the polydisperse polymer, while a corresponding shorter and monodisperse oligomer exhibited an epitaxial 2D crystal structure. In contrast, on the insulating substrate mica, PPE can self-assemble into micrometer-long nanoribbons. Their cross-section was determined quantitatively by scanning force microscopy in tapping mode; this revealed a typical thickness of two molecular layers and a width distribution that is well described by the distribution of molecular weights, according to the Schulz–Zimm distribution. This indicates that the polymers are fully extended in the ribbons and oriented with the conjugated backbone parallel to the substrate and perpendicular to the long axis of the ribbons. Unlike previous studies carried out interfacing single molecules to metallic probes, we propose here functionalised ribbons as polymolecular architectures, which could be used to interconnect gold nanoelectrodes in a molecular-scale electronic device.

Keywords: molecular devices · phenyleneethynylenes · scanning force microscopy · scanning tunneling microscopy · self-assembly

Introduction

The self-assembly of π-conjugated macromolecules on insulating solid substrates offers a strategy for the construction of well-defined and stable nanometer-sized structures with chemical functionalities and physical properties that are of potential use as active components in electronic devices.[1–2] The properties of such molecular devices depend on the structure of the molecular assembly at solid surfaces.[3–6] Intramolecular, intermolecular and interfacial forces are therefore used to obtain highly ordered 1D and 2D polymolecular architectures. Poly(*para*-phenyleneethynylene)s (PPEs)[7] are of particular interest because of their rigid-rod structure,[8, 9] their strongly anisotropic electronic properties, their electroluminescence in the blue-green region[10] and their high and stable photoluminescence quantum yield,[11] which makes it possible to use them for the development of a liquid crystal-based photoluminescent display.[12] The molecular conductivity can be measured directly with scanning tunneling microscopy (STM) by probing the resistance within the self-assembled organic monolayers,[6, 13, 14] by the use of a gold nanocluster as an intermediate contact,[15] by bridging nanoelectrodes with Langmuir–Blodgett layers[16] or through chemisorption of thiol end-functionalised single molecules that can act as molecular-scale alligator clips.[17]

In this paper we report on the first study of molecularly resolved images of a synthetic polydisperse polymer at the solid–liquid interface and on the growth of this macromolecule into molecularly defined ribbons on mica. Scanning tunneling microscopy (STM) and scanning force microscopy (SFM) in tapping mode have been used to elucidate the structures. The molecular arrangement of a *para*-phenyleneethynylene trimer (PE3) on graphite was also investigated as a model system for comparison.

[a] Prof. Dr. J. P. Rabe, Dr. P. Samorí
Humboldt University Berlin, Department of Physics
Invalidenstr. 110, D-10115 Berlin (Germany)
Fax: (+49) 30-20937632
Email: rabe@physik.hu-berlin.de

[b] Prof. Dr. K. Müllen, Dipl.-Chem. V. Francke
Max-Planck-Institute for Polymer Research
Postfach 3148, D-55021 Mainz (Germany)
Fax: (+49) 6131-379350
Email: muellen@mpip-mainz.mpg.de

Results and Discussion

An almost saturated solution of PPE self-assembles at the interface with a highly oriented pyrolytic graphite (HOPG) substrate[27, 28] in a nematic-like molecularly ordered monolayer (Figure 1). The STM image was recorded at constant height and exhibits a 2D molecular pattern of a PPE with an average contour length of 7.9 nm, as obtained from ^{1}H NMR end-group analysis. Both the conjugated skeletons and the

  0947-6539/99/0508-2312 $ 17.50+.50/0

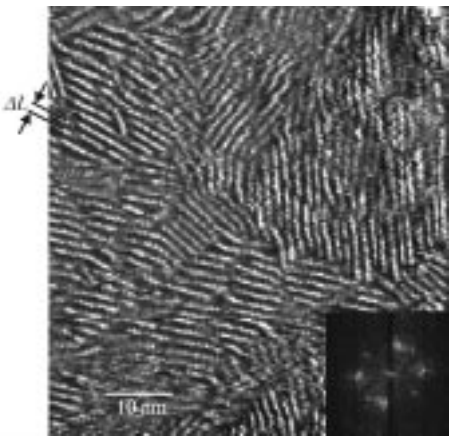

Figure 1. STM current image of **6** in phenyloctane at the interface between the basal plane of graphite and the organic solution ($U_t = 1.2$ V, average $I_t = 1.0$ nA). The molecular backbones exhibit a nematic orientation along preferred directions, as evidenced by the hexagonal pattern in the 2D-Fourier transform. The distance between the backbones, averaged over several images, amounts to $\Delta L = (1.62 \pm 0.10)$ nm.

hexyl side groups lie flat on the (001) plane of the HOPG. The conjugated backbones appear brighter than the aliphatic chains because of a stronger current. This is caused by a relatively small energy difference between the electronic states of the substrate and the adsorbate, while the lower current through the aliphatic part of the molecules is caused by a larger energy difference.[29] The 2D molecular arrangement is composed of domains with specific molecular orientations. The conjugated skeletons are aligned along preferred directions, according to the three-fold symmetry of the HOPG lattice, as visualised by the hexagonal spots in the 2D Fourier transform (Figure 1). The stiffness of the molecular rods[7, 8] and a low polydispersity allows the molecules to pack into this 2D structure and, therefore, play a key role for achieving this true molecular resolution imaging of the synthetic macromolecule. A finite mobility of the nanorods was also detected; this reveals that molecules at the domain boundaries change their tilt angle with respect to the underlying substrate. This molecular dynamics occurs on the timescale of several minutes and can be attributed to a Ostwald ripening process,[30] which is governed by a minimisation of line energies. In addition, the high-resolution imaging made it possible to visualise defects within the organic layer. Moreover, the spacing between neighbouring parallel backbones, which can be attributed to the width of the molecules, amounts to $\Delta L = (1.62 \pm 0.10)$ nm. It is considerably smaller than the 1.9 nm calculated for the case with the alkyl chains extended.[20] This indicates that the side-chains are disordered between adjacent parallel backbones, since an interdigitation of the hexyl groups can be excluded because of steric hindrance.

In comparison, the PE3 oligomer assembles at the solid–liquid interface in an epitaxial 2D crystal structure (Figure 2). In this case the distance between the backbones amounts to

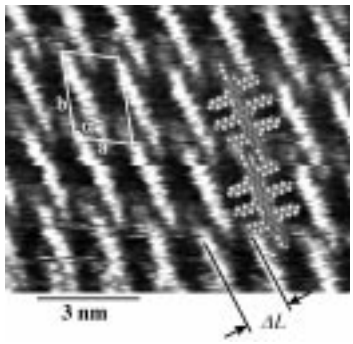

Figure 2. STM current image of **9** in phenyloctane imaged at the solid–liquid interface on HOPG ($U_t = 1.2$ V, average $I_t = 1.0$ nA). 2-D crystal structure with its unit cell, averaged over several images, amounts to $a = (1.78 \pm 0.09)$ nm, $b = (2.90 \pm 0.18)$ nm, and $\alpha = (113 \pm 5)^\circ$. The distance between neighbouring backbones is, in this case, $\Delta L = (1.46 \pm 0.11)$ nm.

$\Delta L = (1.46 \pm 0.11)$ nm, which is in fairly good agreement with the distance obtained for the polymer; this also confirms the hypothesis that the hexyl side-chains are disordered between neighbouring backbones. The difference in the 2D structure of a monodisperse oligomer and a polydisperse polymer, which, on average, is almost three times as long as the trimer, can be attributed to the distribution of molecular lengths; this prevents the assembly of the macromolecules into perfect crystals. Furthermore, the interdigitation of the end-groups, as evident in the trimer (Figure 2), hinders the formation of the columnar phase observed for mixtures of alkanes of different lengths which had been self-assembled on HOPG.[31] The time

Abstract in Italian: *Questo articolo descrive la crescita all' interfaccia fra substrati cristallini e soluzioni di nuovi poli(para-fenileneetinileni) (PPE) funzionalizzati sulle terminazioni della catena principale. Con la Miscoscopia ad Effetto Tunnel (STM) è stata raggiunta una risoluzione molecolare che ha permesso di visualizzare l' organizzazione strutturale delle macromolecole del PPE all' interfaccia tra il piano basale della grafite e una loro soluzione organica. Questo polimero polidisperso è stato così visto in una struttura bidimensionale con un ordine di tipo nematico. Sulla stessa grafite un corrispondente oligomero monodisperso e di lunghezza inferiore è stato invece rivelato assumere una struttura epitassiale, bidimensionale e cristallina . Su un substrato non conduttore come la mica il PPE può invece assemblarsi in nanonastri con lunghezze nella scala dei micrometri. La loro sezione è stata determinata quantitativamente mediante la Microscopia a Scansione di Forza (SFM), nella versione Tapping Mode: il loro spessore è quello di due strati molecolari e la distribuzione delle loro larghezze è in buon accordo con la distribuzione dei pesi molecolari prevista dalla distribuzione di Schulz – Zimm. Questo indica che all' interno del nanonastro i polimeri sono completamente stirati e orientati con la catena coniugata parallela al substrato e perpendicolare all' asse lungo del nanonastro. Proponiamo questi nastri funzionalizzati come architetture polimolecolari pronte ad interconnettere nanoelettrodi di oro in un dispositivo elettronico su scala molecolare, in alternativa all' approccio seguito da studi compiuti in precendenza in cui singole molecole erano interfacciate a sonde metalliche.*

required to achieve the molecular resolution imaging is much longer for the polymer; this is probably caused by self-segregation and consecutive adsorption phenomena that occur at the molecular level, which enables the molecules with different lengths to pack locally well on the substrate.

On the other hand, PPE solutions were also cast onto freshly cleaved mica surfaces. After complete evaporation of the solvent, the morphology of the dry samples was found to depend on the molecular weight (Figure 3 and Table 1). For polymers A – D, with an average of 9, 11, 20 or 22 repeating units and a concentration of the applied solution lower than 0.15 g L^{-1}, ribbons were observed (Figure 3a). Higher molecular weights (samples E and F) led to a grainy morphology (Figure 3c). Figures 3a and 3b show ribbon heights on mica of $h = (2.9 \pm 0.7)$ nm, as determined from 422 ribbons on different samples. From the comparison of this value with the spacing between neighbouring backbones evaluated from molecularly resolved STM images, we suggest that the ribbons are typically two monolayers thick with their alkyl chains oriented perpendicular to the substrate (Figure 4). There are also some sections with single, triple and even higher multilayers. The widths of the ribbons are constant for some straight ribbon sections; however, they are not constant for the whole sample. The apparent widths (number counting) determined from SFM images of samples A – D are shown in Figure 5. These widths need to be corrected for the broadening effect, which is a consequence of the finite radius of the tip.[22, 32] By using a model based on a spherical tip and a rectangular cross-section of the ribbon, the broadening is given by Equation (1).[33]

$$2\Delta = 2\sqrt{h(2R - h)} \quad (1)$$

For the present ribbon height of $h = (2.9 \pm 0.7)$ nm and a terminal radius of the commercial Si tips of $R = (13 \pm 7)$ nm, $2\Delta = (16 \pm 7)$ nm. The true ribbon width, with a 7 nm error bar, is then obtained by subtracting 2Δ from the apparent width.

The peaks of the width distributions shift to higher values with increasing length of the polymer (Figure 5). Since the absolute value of the width is of the order of the length of a single molecule, it is concluded that the extended molecules are packed parallel to each other with their long molecular axis perpendicular to the long ribbon axis, as represented in Figure 4. The distribution of the ribbon widths is attributed to the distribution of molecular weights, which implies that mol-

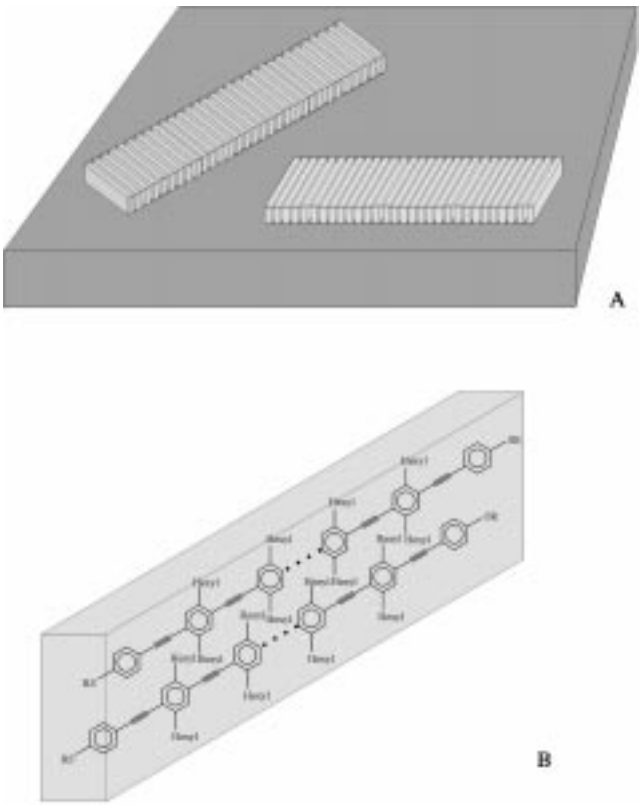

Figure 4. Schematic representation of molecular ribbons adsorbed on the mica surface. A) Ribbons are made of several rods packed parallel one to each other. B) Each rod is typically made of two PPE molecules packed with the hexyl lateral chains perpendicular to the basal plane of the substrate.

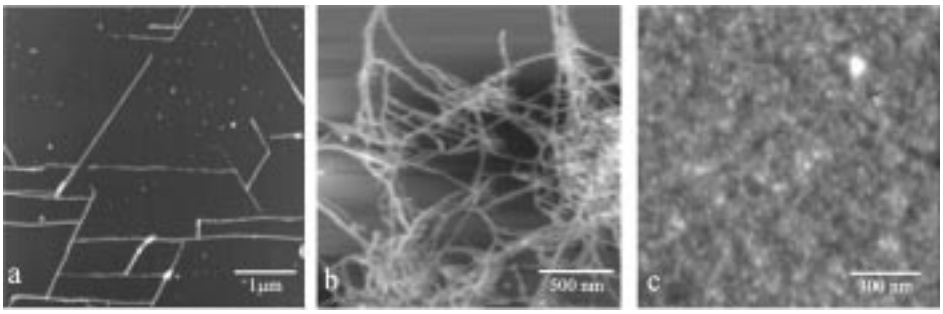

Figure 3. SFM tapping mode height images representing the evolution of the morphology of the PPE as a function of the polymer length. Contour length of the molecule according to ^{1}H NMR results: a) 7.9 nm, b) 16.4 nm, c) 20.3 nm. Height range of images: a) 20 nm, b) 30 nm, c) 20 nm. Solvents: a mixture of THF and phenyloctane was used for a), and pure THF was used for b) and c).

Table 1. PPE samples investigated.[a]

	A	B	C	D	E	F
no. of repeating units	9	11	20	22	28	42
type of PPE	**6**	**6**	**2**	**6**	**6**	**6**
contour length of molecule	7.9 nm	9.2 nm	13.5 nm	16.4 nm	20.3 nm	29.4 nm
M_w/M_n	1.92	3.68	3.82	2.65	2.59	8.23
morphology at low concentration	ribbons	ribbons	ribbons	ribbons	grains	grains

[a] Number of repeating units and contour lengths according to ^{1}H NMR results; type of PPE according to Schemes 1 and 2; polydispersity (M_w/M_n) from GPC measurements with PPP calibration.

0947-6539/99/0508-2314 $ 17.50+.50/0 *Chem. Eur. J.* **1999**, *5*, No. 8

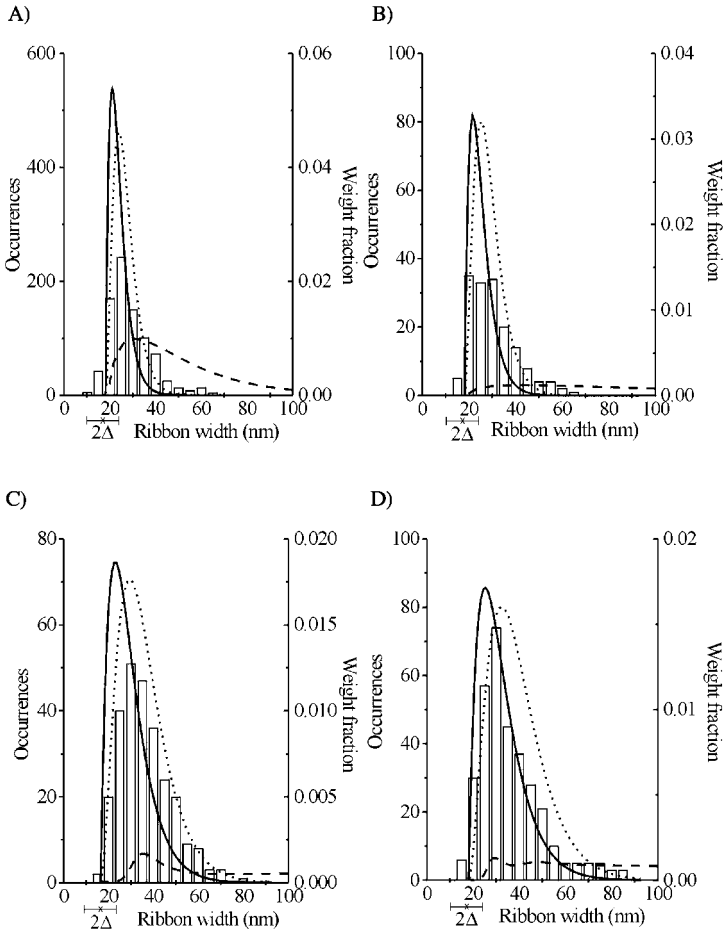

Figure 5. Histograms of the distribution of ribbon widths for PPE batches A–D with increasing length. Contour length of the molecule according to ^{1}H NMR results (Table 1) and number of ribbons measured (given in parentheses): A) 7.9 nm (846), B) 9.2 nm (160), C) 13.5 nm (264), D) 16.4 nm (334). The Schulz–Zimm distribution is plotted in terms of number counting (solid lines) and weight function (dotted line). $2\Delta = (16 \pm 7)$ nm is the effective broadening of the tip.[33] The experimental GPC data (PS calibration) is given as dashed lines.

ecules with similar molecular weights phase-segregate into ribbon sections with homogeneous widths. This segregation phenomenon, which governs the formation of the ribbons, requires a small degree of polymerisation (DP) (Figure 3) and is likely to be favoured by a low macromolecular polydispersity.

Attempts to directly determine the molecular structure by electron diffraction were not successful, probably because of the small amount of material in a given ribbon. However, in *continuous* films of polydiacetylene[34, 35] and poly(*para*-phenyleneethynylene) derivatives[36] similar molecular architectures have been observed.

The polycondensation reaction used for the PPE synthesis gives a molecular-weight distribution which is theoretically described by the Schulz–Zimm distribution.[37] This function was computed for samples A–D in terms of molecular contour lengths by assuming the number-average DP according to the number of repeating units estimated by ^{1}H NMR spectroscopy (Table 1). The mole-fraction distribution is given by Equation (2), while the weight-fraction distribution is given by Equation (3), where $y = k/DP$, k is the degree of coupling (in this case $k = 2$), r is the number of monomers (independent parameter) and $\Gamma(k)$ is the gamma function.

$$F(r) = y^k r^{k-1} \frac{e^{-yr}}{\Gamma(k)} \quad (2)$$

$$W(r) = y^{k+1} r^k \frac{e^{-yr}}{\Gamma(k+1)} \quad (3)$$

These distributions were plotted on the histograms of Figure 5, after being shifted on the x axis by the tip-broadening effect of 16 nm. This made it possible to relate the estimated molecular lengths to the ribbon widths. It is worth noting that there is a good agreement between the mole-fraction distribution and the distribution of ribbon widths.

This match also demonstrates that SFM on these nanostructures may provide a reasonable evaluation of the molecular-weight distributions for a rigid-rod polymer. This is of significance, since, as a result of the commonly observed aggregation of polymer chains, it is difficult to determine the correct molecular-weight distributions for rigid-rod polymers with standard analytical techniques, such as gel permeation chromatography (GPC). The dashed curves in Figure 5 represent the experimental data from GPC measurements (PS calibrated) obtained for the respective polymer. A long tailing of the molecular-weight distribution curve towards high values is observed in the elugrams of the polymers; this drastically increases the polydispersity but has only a minor effect on M_n. A reasonable agreement between the theoretical Schulz–Zimm plot and the experimental GPC curve is observed only for the shortest PPE (Figure 5a). In fact, as the chain length increases the aggregation of the molecules becomes more intense (Figure 5b–d). Moreover, the values are affected by the adsorption of the stiff molecules to the column. Additionally, the protected thiol end-groups enhance this phenomenon in the present case.[18]

A comparison between the different methods used to determine the molecular-weight distributions [^{1}H NMR, GPC (calibrated with PS and PPP)] has shown that M_n evaluated with PPP-calibrated GPC are overestimated on average by 42% with respect to the ^{1}H NMR data. In the case of PS-calibrated GPC, the overestimation is even greater. The polydispersity (M_w/M_n) measured by GPC is 50% larger for PS calibration than that measured with PPP calibration, while M_w is twice as large. This confirms that for the determination of the DP and M_n of a stiff polymer ^{1}H NMR analysis on the end-groups is a suitable technique, while for the approximation of the M_w and polydispersity by GPC, calibration with a rigid-rod polymeric standard like PPP should be used.

Conclusions

We have characterised the self-assembly of a conjugated polymer, PPE, from the molecular scale to its polymolecular architecture. At the interface between graphite and an organic solution a nematic-like molecularly ordered monolayer is formed, whereby both the aliphatic side-chains and the backbones lie flat on the substrate. On mica the conjugated skeletons are also packed parallel to the basal

plane, but the lateral chains are placed perpendicular to it giving rise to self-assembled nanoribbons with a molecular cross-section. SFM imaging of these nanostructures may be used to evaluate the molecular-weight distribution for a rigid-rod polymer. The molecules in the nanoribbons have an average length that has been varied up to 16.4 nm, and they have end-groups that can be deprotected to exhibit thiol functions. Upon doping, such polymolecular units on an insulating substrate may be used as molecular nanowires interfaced with gold nanoelectrodes,[38] either parallel to the conjugated chains or parallel to the long axis of the ribbon, in a molecular-scale electronic device.

Experimental Section

Materials: Two different types of PPE, namely α-iodo-ω-[(2,5-dihexyl-4-ethynyl)phenyl]-poly[(2,5-dihexylphenylene-1,4)ethynylene)] (**2**) and α-[[4-[(*N*,*N*′-dimethylcarbamoyl)thio]phenyl]ethynyl]-ω-[4-[(*N*,*N*′-dimethylcarbamoyl)thio]phenyl]-poly[(2,5-dihexylphenylene-1,4)ethynylene)] (**6**), were synthesised by efficient Pd-catalysed coupling of the AB-monomer 4-ethynyl-2,5-dihexyliodobenzene (**1**).[18] The procedure involves the coupling of the AB-monomer under $[Pd(PPh_3)_4]$/CuI catalysis according to Hagihara's method,[19] followed by the addition of excess 4-[(*N*,*N*′-dimethylcarbamoyl)thio]iodobenzene (**3**) as the end-capping reagent (Schemes 1 and 2). After the work-up procedure, which is necessary in order to remove the remaining end-capping reagent, the iodine function of the resulting α-iodo-ω-[4-[*N*,*N*′-dimethylcarbamoyl)-thio]phenyl]-poly[(2,5-dihexylphenylene-1,4)ethynylene] (**4**) was coupled with 4-ethynyl-[(*N*,*N*′-dimethylcarbamoyl)thio]benzene (**5**) under the same conditions as described above to yield **6**. Furthermore α-Phenylethynyl-ω-phenyl-ter[(2,5-dihexylphenylene-1,4)ethynylene)] (**9**, PE3), was also synthesised by efficient Pd-catalysed coupling of 1,4-diethynyl-2,5-dihexylbenzene (**7**) with 2,5-dihexyl-4-[(trimethysilyl)ethynyl]iodobenzene (**8**) under Hagihara conditions (Scheme 3).

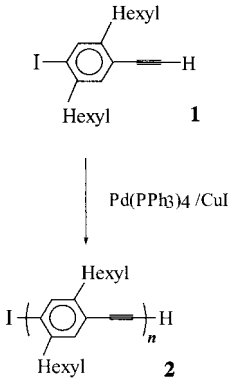

Scheme 1. Synthesis of PPE **2**.

Molecular-weight distributions: The average degree of polymerisation, *DP*, were determined by ^{1}H NMR end-group analysis and gel permeation chromatography (GPC). ^{1}H NMR spectroscopy proved complete end-functionalisation of the PPEs within the limits of experimental error. This method can, therefore, be used to evaluate *DP* and consequently the number-average molecular weight, M_n, by integrating the relative signals of the end-groups and those of the main chain. The ^{1}H NMR spectrum of **2** exhibits proton signals of the terminal repeating unit that bears the iodine atom at $\delta = 7.69$ and 7.30. Polymer **6** exhibits a signal of the methyl groups in the dimethylthiocarbamoyl function at $\delta = 3.02$ and the aromatic protons at $\delta = 7.48$. The main chain signal of the aromatic protons for both **2** and **6** appears at $\delta = 7.36$. Nominal contour lengths of the molecules have been calculated from the determined *DP*s by means of literature values for the length of the repeat unit.[20]

GPC was used to determine the mass-average molecular weight (M_w), in addition to M_n, *DP* and the polydispersity of the polymers **2** and **6**. However, this method is very sensitive to the calibration standards. Since polystyrene (PS) exhibits a different structure and stiffness from PPE, we also used as a rigid-rod macromolecule as the calibration standard, namely a substituted poly(*para*-phenylene) (PPP) with a known molecular weight.[21]

Scanning force microscopy: Muscovite mica slices were cut into discs with a punch and die set in order to produce readily cleavable edges. Solutions

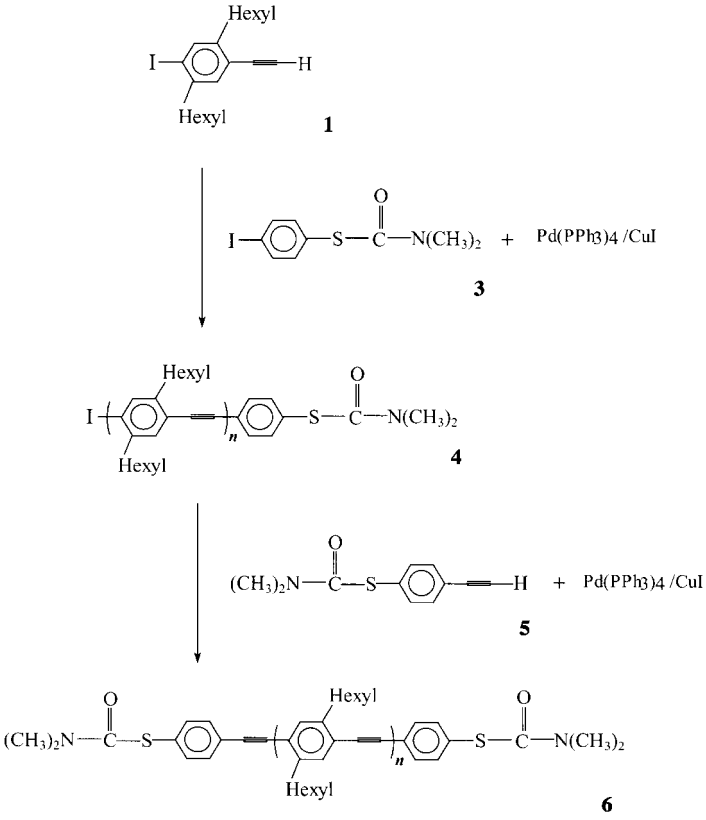

Scheme 2. Synthesis of PPE **6**.

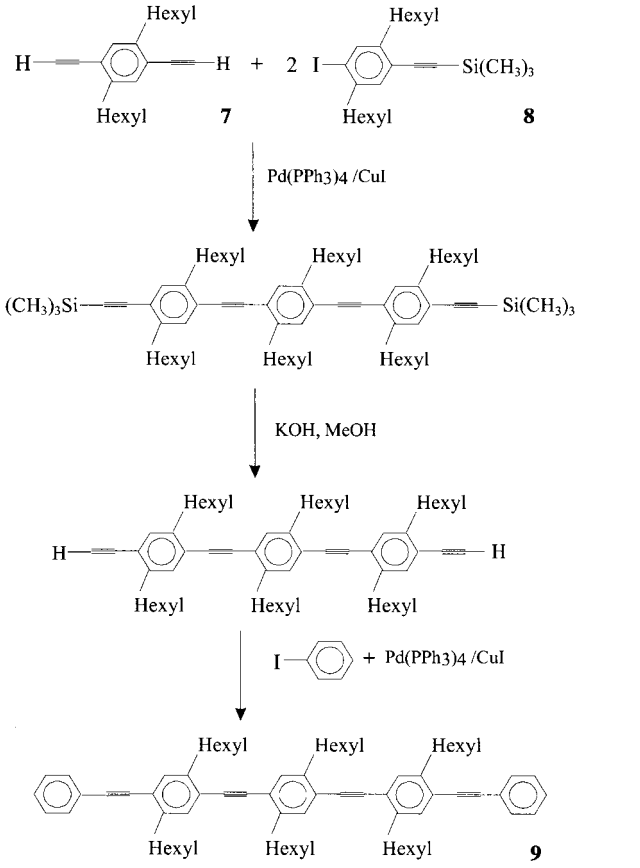

Scheme 3. Synthesis of the *para*-phenyleneethynylene trimer **9**.

0947-6539/99/0508-2316 $ 17.50+.50/0 *Chem. Eur. J.* **1999**, *5*, No. 8

with different concentrations (from 3.0 $g L^{-1}$ to 0.01 $g L^{-1}$ of PPE in pure THF or a mixture of THF and 1-phenyloctane) and different molecular weights were used. Molecular self-assembly was achieved by applying a drop of solution onto a freshly cleaved mica surface and allowing the solvent to evaporate. The size of the homogeneous ribbon sections depends on details of the preparation, including the solvent; this will be discussed elsewhere. The dry samples were investigated by SFM in the tapping mode[22, 23] with the E-scanner[24] in a range of scan lengths from 10 μm to 0.3 μm, and commercial Si cantilevers (length 125 μm and width 30 μm) with a spring constant between 17 and 64 $N m^{-1}$ (Digital Instruments, Santa Barbara, CA). For the calibration of the distance of the piezo controller, images of mica and gold calibration gratings were routinely employed. The ribbon widths were measured[25] from images with a resolution of 512×512 pixels and scan lengths ≤ 3 μm, while their heights were determined by the use of the facilities of the Nanoscope software. Several tens of images were processed for each polymer length in order to minimise the influence of the choice of sample area and to reduce the statistical error.

Scanning tunnelling microscopy: The STM investigation was performed with a home-made[26] beetle-type low-current STM interfaced to Omicron Electronics (Omicron Vakuumphysik GmbH, Germany). Crystalline powder of PPE or PE3 was dissolved in 1-phenyloctane and a drop of the almost saturated solution was applied to the freshly cleaved, highly oriented pyrolytic graphite (HOPG) substrate.[27] This enabled us to measure over a period of several hours with the tunnelling tip immersed in the solution. Molecular resolution at the solid–liquid interface was achieved by means of high scan rates ($\approx 60-100$ Hz $line^{-1}$). By varying the tunnelling parameters it was possible to visualise the HOPG lattice underneath and therefore to calibrate the piezo in situ. The tunnelling tips were electrochemically etched with KOH (2 N) + NaCN (6 N) from a 0.25 mm Pt/Ir (80:20) wire. Unit cells and backbone spacings were averaged on several images after their correction for the piezo drift.

Acknowledgments

We thank Drs. W. Stocker and B. L. Schürmann for useful discussions, and Dr. T. Mangel for the synthesis of one PPE. This work was supported by TMR project SISITOMAS. P.S. acknowledges the EU for a TMR grant.

[1] J.-M. Lehn, *Science* **1993**, *260*, 1762–1763.
[2] P. Bäuerle, *Adv. Mater.* **1993**, *5*, 879–886.
[3] P. Bäuerle, T. Fischer, B. Bidlingmeier, A. Stabel, J. P. Rabe, *Angew. Chem.* **1995**, *107*, 335–339; *Angew. Chem. Int. Ed. Engl.* **1995**, *34*, 303–307.
[4] F. Biscarini, R. Zamboni, P. Samorí, P. Ostoja, C. Taliani, *Phys. Rev. B* **1995**, *52*, 14868–14877.
[5] A. Stabel, P. Herwig, K.Müllen, J. P. Rabe, *Angew. Chem.* **1995**, *107*, 1768–1770; *Angew. Chem. Int. Ed. Engl.* **1995**, *34*, 1609–1611.
[6] L. A. Bumm, J. J. Arnold, M. T. Cygan, T. D. Dunbar, T. P. Burgin, L. Jones, II, D. L. Allara, J. M. Tour, P. S. Weiss, *Science* **1996**, *271*, 1705–1707.
[7] R. Giesa, *J. Macromol. Sci Rev. Chem. Phys.* **1996**, *C36*, 631–670.
[8] M. Moroni, J. Le Moigne, S. Luzzati, *Macromolecules* **1994**, *27*, 562–571.
[9] P. Wautelet, M. Moroni, L. Oswald, J. Le Moigne, A. Pham, J.-Y. Bigot, S. Luzzati, *Macromolecules* **1996**, *29*, 446–455.
[10] K. Tada, M. Onoda, M. Hirohata, T. Kawai, K. Yoshino, *Jpn. J. Appl. Phys.* **1996**, *35*, L251–L253.
[11] C. Weder, M. S. Wrighton, *Macromolecules* **1996**, *29*, 5157–5165.
[12] C. Weder, C. Sarwa, A. Montali, C. Bastiaansen, P. Smith, *Science* **1998**, *279*, 835–837
[13] R. Heinz, J. P. Rabe, *Langmuir* **1995**, *11*, 506–511 and 2857.
[14] S. Datta, W. Tian, S. Hong, R. Reifenberger, J. I. Henderson, C. P. Kubiak, *Phys. Rev. Lett.* **1997**, *79*, 2530–2533.
[15] R. P. Andres, T. Bein, M. Dorogi, S. Feng, J. I. Henderson, C. P. Kubiak, W. Mahoney, R. G. Osifchin, R. Reifenberger, J. M. Tour, *Science* **1996**, *272*, 1323–1325.
[16] S. J. Tans, R. Miedema, L. J. Geerlings, C. Dekker, J. Wu, G. Wegner, *Synth. Met.* **1997**, *84*, 733–734.
[17] M. A. Reed, C. Zhou, C. J. Muller, T. P. Burgin, J. M. Tour, *Science* **1997**, *278*, 252–253.
[18] V. Francke, T. Mangel, K. Müllen, *Macromolecules* **1998**, *31*, 2447–2453.
[19] a) K. Sonogashira, Y. Tohda, N. Hagihara, *Tetrahedron Lett.* **1975**, 4467; b) H. A. Dieck, R. F. Heck, *J. Organomet. Chem.* **1975**, *93*, 259.
[20] Discover Version 4.0.0, Biosym Technologies, San Diego, CA.
[21] S. Vanhee, R. Rulkens, U. Kehmann, C. Rosenauer, M. Schulze, W. Köhler, G. Wegner, *Macromolecules* **1996**, *29*, 5136–5142.
[22] C. Bustamante, D. Keller, *Physics Today* **1995**, *48*, 12, 32–38.
[23] J. Tamayo, R. Garcia, *Langmuir* **1996**, *12*, 4430–4435.
[24] Nanoscope III Multimode, Digital Instruments, Santa Barbara, CA.
[25] Software package Image Tools 1.27, developed by the University of Texas—Health Science Center in San Antonio, was used to measure the ribbon widths one-by-one with a ruler.
[26] P. E. Hillner, J. F. Wolf, J. P. Rabe, Humboldt University Berlin.
[27] J. P. Rabe, S. Buchholz, *Science* **1991**, *253*, 424–427.
[28] P. G. M. Grum, S. De Feyter, A. Gesquière, P. Vanoppen, M. Rücker, S. Valiyaveettil, G. Moessner, K. Müllen, F. De Schryver, *Angew. Chem* **1997**, *109*, 2713–2715; *Angew. Chem Int. Ed. Engl.* **1997**, *36*, 2601–2603.
[29] R. Lazzaroni, A. Calderone, J. L. Brédas, J. P. Rabe, *J. Chem. Phys.* **1997**, *107*, 99–105.
[30] A. Stabel, R. Heinz, F. C. De Schryver, J. P. Rabe, *J. Phys. Chem.* **1995**, *99*, 505–507.
[31] R. Hentschke, L. Askadskaya, J. P. Rabe, *J. Chem. Phys.* **1992**, *97*, 6901–6909.
[32] H-J. Butt, R. Guckenberger, J. P. Rabe, *Ultramicroscopy* **1992**, *46*, 375–393.
[33] P. Samorí, V. Francke, T. Mangel, K. Müllen, J. P. Rabe, *Opt. Mater.* **1998**, *9*, 390–393.
[34] W. Wang, G. Lieser, G. Wegner, *Liq. Cryst.* **1993**, *15*, 1–24.
[35] K. E. Huggins, S. Son, S. I. Stupp, *Macromolecules* **1997**, *30*, 5305–5312.
[36] D. Ofer, T. M. Swager, M. S. Wrighton, *Chem. Mater.* **1995**, *7*, 418–425.
[37] J. Brandrup, E. H. Immergut, *Polymer Handbook*, 3rd ed., Wiley Interscience **1989**, pp. 275–296.
[38] Gaps in the 10 nm regime between two gold nanoelectrodes on silica have been fabricated by e-beam lithography and characterised electrically and by SFM.

Received: January 13, 1999 [F1539]